Remote Sensing of Environment 156 (2015) 383–394

Contents lists available at ScienceDirect

Remote Sensing of Environment

journal homepage: www.elsevier.com/locate/rse

SMOS soil moisture product evaluation over West-Africa from local to regional scale

Samuel Louvet [a], Thierry Pellarin [a,b], Ahmad al Bitar [d], Bernard Cappelaere [e], Sylvie Galle [a,c], Manuela Grippa [f], Claire Gruhier [d], Yann Kerr [d], Thierry Lebel [a,c], Arnaud Mialon [d], Eric Mougin [f], Guillaume Quantin [a], Philippe Richaume [d], Patricia de Rosnay [g]

[a] University of Grenoble Alpes, LTHE, F-38000 Grenoble, France
[b] CNRS, LTHE, F-38000 Grenoble, France
[c] IRD, LTHE, F-38000 Grenoble, France
[d] Centre d'Etudes Spatiales de la BIOsphère (CESBIO), CNES CNRS IRD UPS, OMP, Toulouse, France
[e] IRD, Hydrosciences Montpellier (HSM), CNRS IRD UM1 UM2, Montpellier, France
[f] Géosciences Environnement Toulouse (GET), UMR 5563 (CNRS IRD UPS), Observatoire Midi-Pyrénées, 14 avenue Edouard Belin, 3100 Toulouse, France
[g] European Centre for Medium-Range Weather Forecasts (ECMWF), Reading, United Kingdom

ARTICLE INFO

Article history:
Received 17 March 2014
Received in revised form 6 October 2014
Accepted 6 October 2014
Available online 5 November 2014

Keywords:
SMOS
Remote sensing
Soil moisture
West-Africa
Rainfall estimation

ABSTRACT

This paper assessed the SMOS soil moisture values from Level 3 (SMOS L3SM) product provided by the French CNES-CATDS. The evaluation was conducted at the local scale through comparison with ground-based soil moisture measurements acquired in Mali, Niger and Benin from 2010 to 2012. The SMOS L3SM product was compared to three other satellite-based soil moisture products. It was found that, in average over the three sites, the SMOS L3SM product provided the best coefficients of correlation and the lowest root mean square errors (RMSE). The second part of the paper is devoted to retrieve soil moisture estimates between successive SMOS soil moisture measurements in order to increase the temporal resolution. The result of the methodology allows obtaining 3-hour soil moisture mapping over West Africa with a coefficient of correlation greater than 0.82, and an RMSE lower than 0.030 $m^3\ m^{-3}$ in Niger and Mali and lower than 0.044 $m^3\ m^{-3}$ in Benin.

1. Introduction

Soil moisture is known to potentially influence atmospheric conditions through its impact on evaporation and other surface energy fluxes (Eltahir, 1998; Fischer, Seneviratne, Vidale, Luthi, & Schar, 2007; Taylor et al., 2011). Land-atmosphere feedbacks were found to be particularly strong in the central Great Plains of North America, the Sahel, equatorial Africa, and India (Koster et al., 2004). The reason is relatively simple: regions with strong land-atmosphere feedbacks require a sufficiently abundant evaporation to act on rainfall but low enough to be controlled by soil moisture, which excludes humid climates as well as too dry climates. Best candidates are regions of transition between wet and dry climates such as the Sahel region. Recent studies investigated the land-atmosphere feedbacks in West Africa (Adler, Kalthoff, & Gantner, 2011; Klupfel, Kalthoff, Gantner, & Kottmeier, 2011) but the complex relationship between soil moisture and atmospheric conditions, and particularly the precipitation, is still to investigate and is probably one reason that explains the current uncertainty of atmospheric general circulation models from IPCC (The Intergovernmental Panel on Climate Change) to predict the evolution of the precipitation regime in West Africa by the end of the century.

In this context, satellite-based soil moisture products are of great interest for providing regularly regional soil moisture maps at the global scale. In November 2009, ESA (European Space Agency) launched the first satellite specifically dedicated to measuring surface soil moisture and ocean salinity. The SMOS (Soil Moisture and Ocean Salinity) mission is a passive interferometric radiometer operating at L-band (1.4 GHz) since passive microwaves remote sensing was shown to be the most efficient approach to provide soil moisture information at the global scale (Kerr, 2007). Although SMOS is the first mission operating at L-band, another significant difference with previous microwave missions is the multi-angular acquisition capability which is used to separate the different contributions (soil and vegetation) to the signal (Kerr, 2007; Wigneron et al., 2007).

Since SMOS launch, several papers were devoted to assess the accuracy of the new SMOS soil moisture retrievals at the global scale (Albergel et al., 2012; Al-Yaari et al., 2014; Leroux, Kerr, Richaume, & Fieuzal, 2013) or in various geographic areas such as over US (Al Bitar et al., 2012; Collow, Robock, Basara, & Illston, 2012; Jackson et al., 2012; Leroux et al., 2014), Europe (Bircher, Skou, Jensen, Walker, & Rasmussen, 2012; dall'Amico, Schlenz, Loew, & Mauser, 2012; Lacava et al., 2012; Montzka et al., 2013; Parrens et al., 2012; Schlenz,

http://dx.doi.org/10.1016/j.rse.2014.10.005
0034-4257/

dall'Amico, Mauser, & Loew, 2012), Australia (Peischl et al., 2012) or Spain (Wigneron et al., 2012). No evaluation of the SMOS soil moisture product was done over Africa except on the extreme North of Africa (Pierdicca, Pulvirenti, Fascetti, Crapolicchio, & Talone, 2013). All these studies were useful to analyze SMOS retrievals accuracy and improve the retrieval algorithm. The principle of the retrieval algorithm is to exploit multi-angular L-band measurements in order to retrieve simultaneously several surface parameters including soil moisture and vegetation characteristics. Regularly, some improvements are made on the retrieval algorithm and are implemented in the operational algorithm. Thus, a complete reprocessing of the SMOS data is done to obtain improved soil moisture and vegetation characteristics time-series. At the moment (January 2014), only one complete reprocess of the SMOS level 3 data was done.

The first objective of this paper is to evaluate the SMOS Level 3 data over West Africa using local measurements from the AMMA-CATCH (African Monsoon Multi-disciplinary Analysis (AMMA)–Couplage de l'Atmosphère Tropicale et du Cycle Hydrologique) observatory (Lebel et al., 2009). The soil moisture network installed between 2005 and 2006 in Mali, Niger and Benin (about 120 soil moisture sensors at various depths) has the advantage to represent a variety of bio-climatic conditions with a strong vegetation gradient (from bare soil to deciduous tropical forest). The use of surface soil moisture measurements (5 cm depth) allows estimating the capability of SMOS to retrieve soil moisture value against a large vegetation optical depth gradient. The study is conducted over West Africa from January 2010 to December 2012. This period allows observing a range of seasonal conditions and contrasted years (2010 and 2011 were respectively abnormally wet and dry on the major part of West-African region). Additionally, an intercomparison with three other existing satellite-based soil moisture products is done. Two of them are based on AMSR-E (Advanced Microwave Scanning Radiometer) sensor onboard the AQUA satellite platform (AMSR-VUA from the University of Amsterdam (Owe, de Jeu, & Holmes, 2008) and AMSR-NSIDC (Njoku, Jackson, Lakshmi, Chan, & Nghiem, 2003)). The last soil moisture product is based on the ASCAT sensor (Advanced SCATterometer) onboard the MetOP satellite platform (Bartalis et al., 2007).

The second objective of the paper is devoted to apply a methodology to derive 3-hour soil moisture mapping based on SMOS daily retrievals. Initially developed for AMSR-E passive microwave measurements (onboard the AQUA satellite platform, C-band, 6.9 GHz), the methodology is applied for the first time to the SMOS soil moisture retrievals. High temporal resolution soil moisture mapping is potentially of great interest for operational applications in West Africa, particularly for flood forecasting, drought monitoring and yield forecasts or to better understand the complex land-atmosphere feedbacks observed in the West Africa region.

2. Study area and data set

2.1. West Africa

The study area spans over 16° in latitude from 4° N to 20° N and 40° in longitude from 20° W to 20° E (Fig. 1). The region exhibits a strong north-south bio-climatic gradient with less than 100 mm of annual precipitation at the North and 1200 to 2000 mm on the coast. To better understand the geophysical processes which govern the evolution of the monsoon and the associated continental water cycle, the AMMA-CATCH long term observing system (www.amma-catch.org) is based on three mesoscale sites sampling the West-African eco-climatic gradient (Cappelaere et al., 2009; Lebel et al., 2009; Mougin et al., 2009; Seguis et al., 2011). Observations started in 1999 (in Benin) and were intensified during the AMMA project in 2005 which enhanced the in situ observing system network.

The three meso-scale sites located in Mali, Niger, and Benin sample the north–south latitudinal gradient and the main vegetation types. During the AMMA project, about 120 soil moisture sensors were installed in Mali, Niger and Benin in 2005–2006. Among these, numerous soil moisture sensors were installed at 5 cm depth for satellite products assessment. The evaluation of the SMOS product will be conducted on the three 0.25° pixels belonging to the super sites in Mali, Niger and Benin (Fig. 1).

Both the Mali and Niger sites are located in the Sahel region characterized by a single rainy season between June and October. The Mali site is located in the Gourma region near the Agoufou village (1.48° W–15.34° N). The vegetation is mainly composed by open woody savannah (Mougin et al., 2009) and the observed annual rainfall in Agoufou was 400 mm in 2010, 482 mm in 2011 and 393 mm in 2012. The Niger site is typical of a large fraction of the cultivated Sahel area. This site is close to the Wankama village centered on 13.645° N–2.632° E. The annual rainfall amount observed in the Wankama region was 401 mm in 2010, 362 mm in 2011 and 511 mm in 2012. Niger site is mainly composed of tiger bush on the plateaus, fallow savannah and pearl millet crop fields on the sandy slopes (Cappelaere et al., 2009). The Benin site is located 400 km south of the Niger site and differs from the two previous sites. It belongs to the Ouémé catchment (1.5–2.8° E; 9–10.2° N) which covers about 15,000 km^2 (Seguis et al., 2011). Most of ground-based instruments are located in the North–West part of the Ouémé catchment (9.745° N–1.653° E). At such latitudes the climate is no longer Sahelian but Soudanian. The observed annual rainfall amount was 1578 mm in 2010, 1093 mm in 2011 and 1512 mm in 2012. With more water available, the vegetation is significantly denser than at higher latitudes. Woody savannah and tropical forest are typical vegetation of this site.

2.2. Ground-based soil moisture measurements

Most of ground-based soil moisture sensors were installed through a vertical sampling to capture the rooting zone profile. In the present study, only soil moisture probes located at 5 cm depth are considered according to the assumed penetration depth of 0–2 cm or 0–3 cm at L-band (Escorihuela, Chanzy, Wigneron, & Kerr, 2010). Geographical coordinates of soil moisture stations as well as land-cover type and depth of available soil moisture probes are presented in Table 1 and localization of soil moisture stations within satellite 0.25° pixels is illustrated in Fig. 1. In the Benin site, soil moisture stations were installed at various locations along three hill slopes (catena) covered with forest, crops and savanna respectively. In Niger, three sites were installed and each of them includes 2 soil moisture probes at 5 cm depth. In Mali, due to geo-political events which occurred in 2011 and 2012 in North Mali, we only use the Agoufou station where two soil moisture profiles were installed on top and bottom of a hill slope. To resume, we used 2 sensors in the Mali site and 6 sensors in both Niger and Benin sites respectively. Note that the AMMA-CATCH soil moisture network was previously used for various studies related to satellite product assessment (Baup, Mougin, de Rosnay, Timouk, & Chenerie, 2007; Baup et al., 2007, 2011; de Rosnay et al., 2009; Fatras, Frappart, Mougin, Grippa, & Hiernaux, 2012; Gruhier et al., 2008, 2010; Pellarin, Louvet, Gruhier, Quantin, & Legout, 2013; Pellarin et al., 2009a; Pellarin et al., 2009b; Zribi et al., 2009).

The evaluation of satellite surface soil moisture products can be done using comparisons between point-scale ground observations and footprint-scale (40×40 km^2) retrievals. However, since the majority of the available ground-based soil moisture observations are from low-density networks in which one or two measurements are available per satellite footprint, various authors investigated the spatial sampling errors in coarse-scale soil moisture estimates derived from point-scale observations (Brocca, Tullo, Melone, Moramarco, & Morbidelli, 2012; Cosh, Jackson, Bindlish, & Prueger, 2004; Loew & Schlenz, 2011; Miralles, Crow, & Cosh, 2010). Different approaches were assessed to

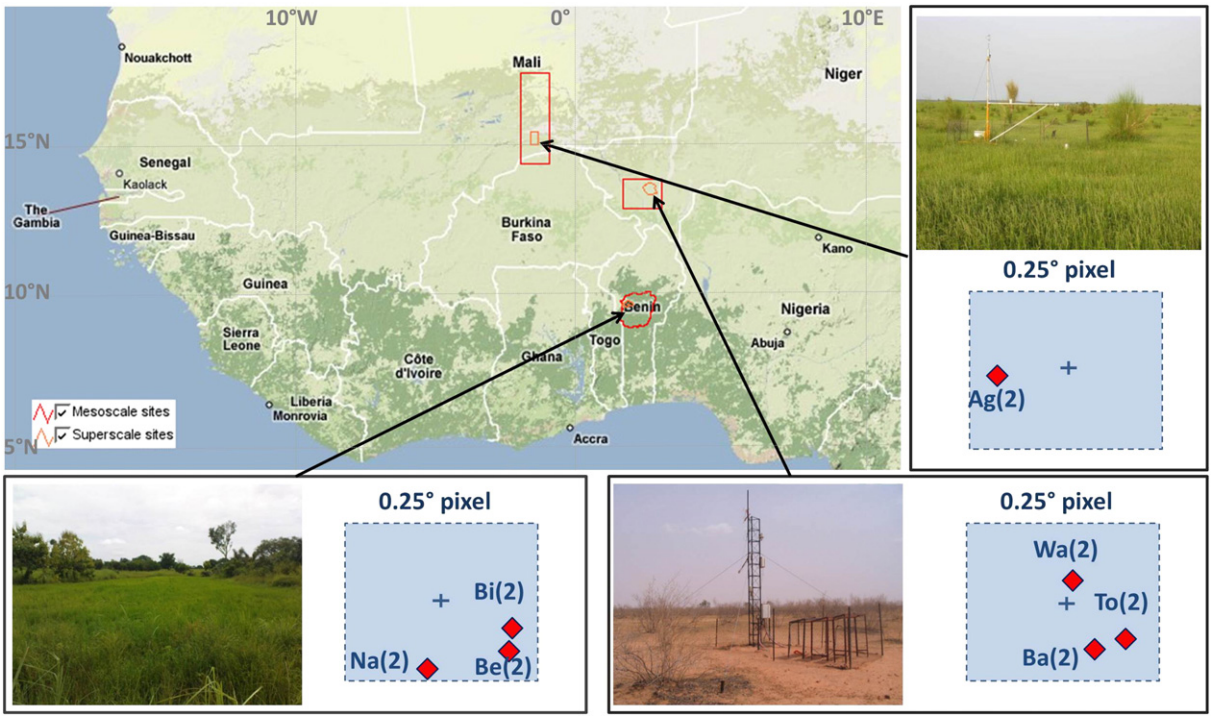

Fig. 1. Localization of the three meso-scale sites in Benin, Mali and Niger where in-situ soil moisture stations are installed. Blue boxes show the three considered EASE-Grid SMOS pixels used for the comparison with in-situ soil moisture stations illustrated with red diamonds.

infer the error of the satellite product from the uncertainties associated to the up-scaling of in situ soil moisture observations showing that the point-to-area sampling error is generally very low and concluded that it is feasible to validate satellite footprint-scale soil moisture products using existing low-density ground networks. In the present study, as we have several measurements in each site, the average value of all soil moisture measurements within the SMOS 0.25° pixel was expected to represent the best-available approximation of the footprint soil moisture estimate at the ground level.

2.3. SMOS CATDS products

The sensor onboard of SMOS satellite is based on interferometric systems with 69 elementary antennas (Kerr et al., 2001). The orbit is heliosynchronous and the sensor is inclinated by 32.5°. SMOS records brightness temperatures at only one frequency (1.4 GHz) but with angular coverage ranging from 0 to 65°, providing a multi-angular information in full stokes. Brightness temperatures are recorded and provided in the antenna frame, also called X and Y polarizations. Brightness temperatures recorded over land surface vary between 200 and 350 K. Soil water content is the main variable through dielectric constant which influences the signal. Without vegetation cover, the range of variation of brightness temperatures is around 230–330 K between a saturated and a very dry soil. The signal refers to the emissivity of the top 2–3 cm of soil at an average spatial resolution of 40 km. The signal can penetrate clouds and the atmospheric effects are very low. The contribution of the vegetation is correlated to the vegetation water content and its influence on the signal is weaker than at C or X-band but has to be accounted for. To derive soil moisture estimates, brightness temperatures are simulated by the L-MEB radiative transfer model (L-band Microwave Emission of the Biosphere, Wigneron et al., 2007). The retrieved soil moisture values are obtained through a minimization technique algorithm (Kerr et al., 2012). In the presence of large fraction of water, ice, or strong topography, the soil moisture value is not retrieved.

The SMOS products evaluated in this study are the Level 3 Brightness Temperature (L3TB) and the Level 3 Soil Moisture (L3SM) products from the CNES CATDS (Centre Aval de Traitement des Données SMOS). These

Table 1
Geographic coordinates, soil depths and land-cover types of all soil moisture probes available in Mali, Niger and Benin sites. Only 5 cm depth soil moisture sensors were used in this study.

	Sites	Latitude	Longitude	Probes depths (cm)	Land-cover
Benin	Nalohou (top)	9.743° N	1.606° E	5, 10, 20, 40, 60, 100	Mixed crops
	Nalohou (middle)	9.745° N	1.605° E	5, 10, 20, 40, 120	Mixed crops
	Belefoungou (top)	9.790° N	1.710° E	5, 10, 20, 40, 60, 100	Forest
	Belefoungou (middle)	9.795° N	1.715° E	5, 10, 20, 40, 50, 100	Forest
	Bira (middle)	9.827° N	1.717° E	5, 10, 20, 40, 60, 80	Savana
	Bira (bottom)	9.828° N	1.716° E	5, 10, 20, 40, 60, 100	Savana
Niger	Wankama	13.646° N	2.632° E	5, 5, 10–40, 40–70, 70–100, 100–130	Millet
	Banizoumbou	13.532° N	2.660° E	5, 5	Fallow
	Tondikiboro	13.548° N	2.696° E	5, 5, 10–40, 40–70, 70–100, 100–130	Fallow
Mali	Agoufou (top)	15.354° N	1.479° W	5, 10, 40, 120, 220	Fallow
	Agoufou (bottom)	15.356° N	1.478° W	5, 30, 60, 120, 150, 250, 400	Fallow

products are presented in the NetCDF format on the EASE (Equal Area Scalable Earth) grid with a 25 km cylindrical projection. The version of the products used is the 2.46 from January 2010 to end October 2012 and 2.50 from November 2012 to end 2012.

The Level 3 Soil Moisture product contains geo-located retrieved soil moisture values (in $m^3\ m^{-3}$) and its associated data quality index (Dqx). In addition, the L3SM product contains useful additional products such as the estimation of the vegetation optical thickness (at nadir), information about potential radio frequency interferences (RFI), simulated TB computed using the forward model at the specific incidence angle of 42.5°, and basically all required information useful to understand the status/configuration of the retrieval. The L3SM product uses the Dobson dielectric permittivity model (Dobson, Ulaby, Hallikainen, & El-Rayes, 1985).

RFI contamination in West Africa is rather weak as can be observed in the web page http://www.cesbio.ups-tlse.fr/SMOS_blog/smos_rfi/. The impact is more significant for ascending orbits due to European and Middle East RFI which can influence the ascending SMOS field of view. Globally, RFI contamination decreases from 2010 to 2012 particularly in the Mauritania region. In Northern Chad region, RFI still remains but with a weaker level.

2.4. Ground-based and satellite-based precipitation measurements

In this study, we used part of the AMMA rain-gauge network located in Niger, Mali and Benin. In agreement with the SMOS L3SM product, we focused on three 0.25° pixels in the EASE-Grid projection where there are numerous soil moisture and rain-gauge sensors. The center coordinates of the three areas are respectively: 13.625° N, 2.625° E (Niger); 15.34° N, 1.48° W (Mali); and 9.625° N, 1.625° E (Benin). On these sites, the kriging technique of Vischel et al. (2011) was carried out using all rain-gauges belonging to a 0.75° square area centered over the three sites. The kriging technique used 17 rain-gauge stations in Mali, 20 rain-gauge stations in Niger, and 21 rain-gauge stations in Benin. It results a 0.01° rainfall map every 5 minutes. Then, a spatial and temporal average value is obtained over the 0.25° × 0.25° area every 3 hours.

In the second part of the present paper, we used three satellite-based precipitation products. Every product is 3-hours time resolution and 0.25° spatial resolution. TRMM-3B42 is an operational product of the Tropical Rainfall Measuring Mission (TRMM) satellite launched in November 1997. This precipitation product is derived from remote sensing data of the TRMM Multi-Satellite Precipitation Analysis (TMPA) computed every 3 hours. The algorithm is based on inter-calibrated and combined precipitation estimates based on TRMM-2A12, SSMI (Special Sensor Microwave Imager), AMSR (Advanced Microwave Scanning Radiometer), AMSU (Advanced Microwave Sounding Unit), and IR (infrared) estimates from geostationary IR observations (Kummerow et al., 2001). CMORPH (CPC MORPHing technique, Joyce, Janowiak, Arkin, & Xie, 2004) produces global precipitation analyses at very high spatial and temporal resolution. This technique uses precipitation estimates that have been derived from low orbiter satellite microwave observations exclusively, and whose features are transported via spatial propagation information that is obtained entirely from geostationary satellite IR data. At present precipitation estimates derived from the passive microwaves aboard the DMSP 13, 14 and 15 (SSM/I), the NOAA-15, 16, 17 and 18 (AMSU-B), and AMSR-E and TMI aboard NASA's Aqua and TRMM spacecraft, are incorporated. Finally, the PERSIANN product (Precipitation Estimation from Remotely Sensed Information using Artificial Neural Networks, Sorooshian et al., 2000) uses a neural network approach to derive relationships between IR and MW data which are applied to the IR data to generate rainfall estimates. The time and space resolutions of these products are respectively 0.25° and 3 hours, although finer resolutions are also available for CMORPH and PERSIANN.

Recently Gosset, Viarre, Quantin, and Alcoba (2013) have compared several satellite based rainfall products over two dense rain gauge networks in West Africa. The real-time products (PERSIANN, TRMM 3B42 RT and CMORPH) have among the highest correlations but exhibit moderate to high positive biases. These biases are steady over the years and are very significant for PERSIANN in Niger, reaching 100–150% of the annual rainfall.

3. SMOS products assessments

3.1. Brightness temperatures

The Level 3 Brightness Temperature product (L3TB) from CATDS is a daily global polarized brightness temperature product, arranged by incidence angle values, in full polarization. It includes all brightness temperatures acquired that day, transformed from original X and Y polarizations (antenna frame) to ground polarization reference frame (H and V polarization).

In order to get a comprehensive idea about the gain of L-band (SMOS) versus existing C-, X- and K-band under various vegetation densities, we computed the standard deviation of TB from May to September 2011 (which corresponds to the rainy season of the major part of sub-Saharian West Africa) for each of the four frequencies (1.4 GHz (SMOS); 6.9, 10.7 and 18.7 GHz (AMSR-E)). In 2010 and 2011, the AMSR-E passive microwave sensor was operating and stopped producing data on 2011 October 4th. Since AMSR-E measurements are acquired at 55° incidence angle, we used the 52.5° incidence angle of SMOS which is a mean value of all incidence angles ranging from 50 to 55°. In addition, only TB without risk of radio frequency interferences (RFI) where computed ($190\ K < TB_H < 320\ K$). Fig. 2 presents the TB standard deviations computed for horizontal polarization measurements for descending orbits. A maximum of variability can be observed in the Sahelian region (10–17° N) for the four data sets. Beyond 17° N, there is almost no precipitation; the dynamic of soil moisture is very weak and leads to low TB dynamic. On the other hand, below 10° N, the low variability of the brightness temperatures is mainly due to the presence of dense vegetation which attenuates the signal from the soil. It can be observed that the SMOS TB shows a greater dynamic (standard deviation between 4 and 15 K) in the Soudanian region (8–11° N) compared to AMSR-E measurements (between 3 and 9 K). In the western part of the Guinean region (below 8° N), the SMOS measurements have a weak dynamic (4–6 K) quite similar to that of AMSR-E at 6.9 GHz.

3.2. SMOS L3SM versus in-situ soil moisture measurements

The first step was to compare SMOS L3 soil moisture estimates with ground-based soil moisture measurements obtained in Mali, Niger and Benin. Results are shown in Fig. 3 for the 2010–2012 period. SMOS values were filtered out from RFI (flag value in L3SM product) as well as uncertain inversions ($Dqx < 0.04\ m^3\ m^{-3}$). The different climates between the three sites can be clearly observed on the time-series of surface soil moisture. Mali and Niger ground-based measurements exhibit a typical seasonal cycle of the Sudano–Sahelian area with a distinct wet season from June to October. The soil moisture evolution is different in Benin with a wetter and longer monsoon period.

As stated in Section 2.2, all 5-cm soil moisture probes located at the three selected 0.25 × 0.25° areas in Niger, Mali and Benin were averaged in order to be as much as possible representative of the soil moisture at the 0.25x0.25° scale. Thus, Fig. 3 shows the averaged value (continuous black line) as well as the range of minimum and maximum values of all sensors (gray area, i.e. 2 stations in Mali, 6 stations in Niger and 6 stations in Benin).

To assess the accuracy of the SMOS soil moisture product, we computed three statistical scores: the coefficient of correlation (R), the root mean square error (RMSE) and the bias. Regarding the

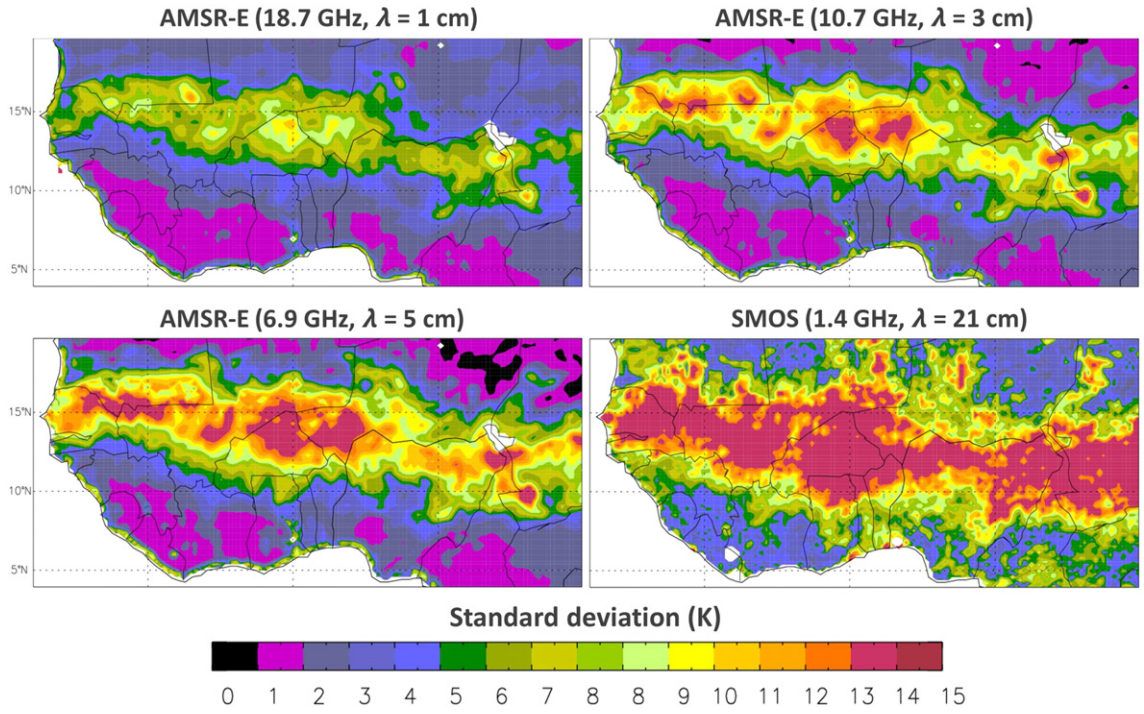

Fig. 2. Standard deviation of H-pol brightness temperatures (AMSR-E and SMOS) observed between May and October 2011 for four frequencies: 18.7 GHz, 10.7 GHz, 6.9 GHz and 1.4 GHz.

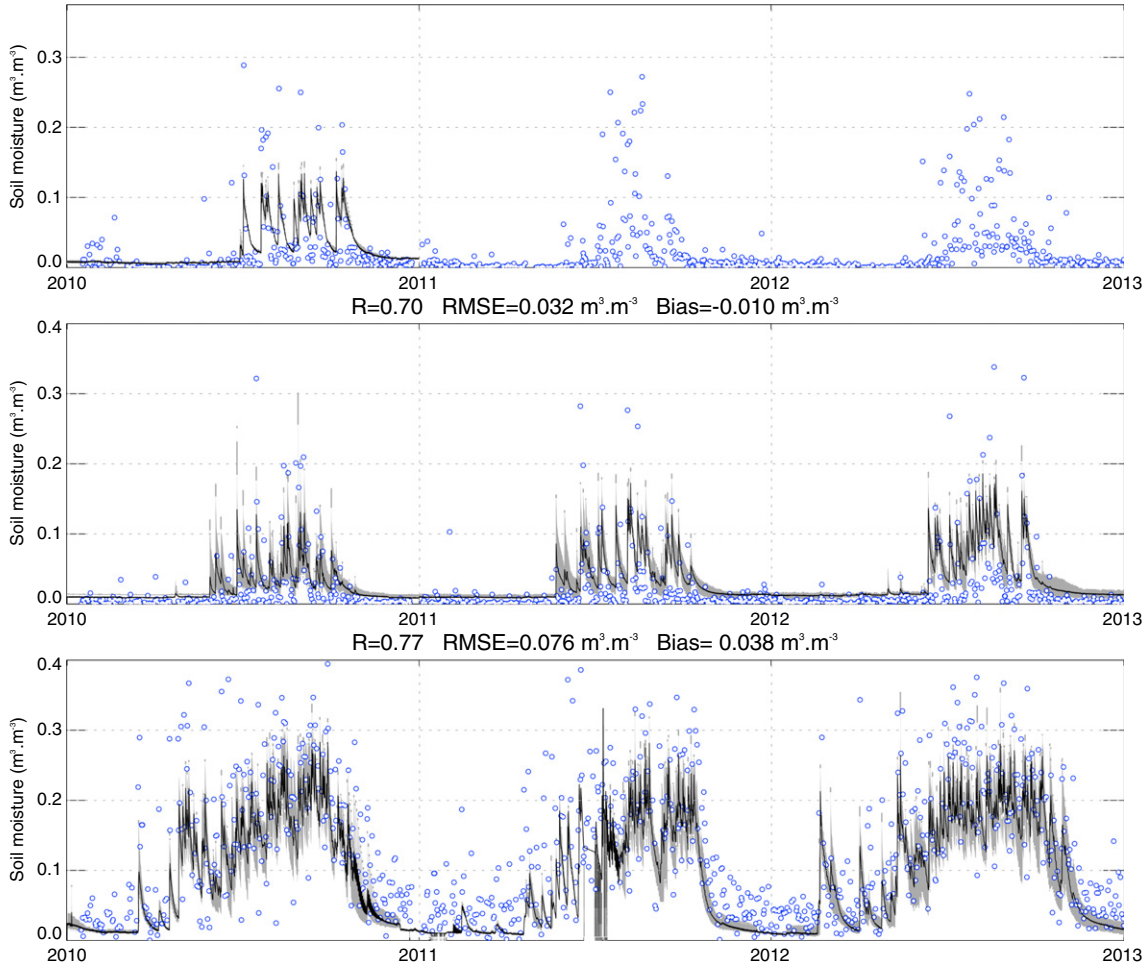

Fig. 3. Observed in-situ surface soil moisture (black curve) versus SMOS surface soil moisture estimates (open circles) at the Mali (top), Niger (middle) and Benin (bottom) sites.

coefficient of correlation, the R score is 0.74, 0.70 and 0.77 respectively for the Mali, Niger and Benin sites. RMSE scores were found to be better than the SMOS expected soil moisture retrieval accuracy (fixed to 0.04 $m^3\ m^{-3}$) in the Niger and Mali sites (0.033 $m^3\ m^{-3}$ and 0.032 $m^3\ m^{-3}$ respectively). However, the RMSE score in the Benin site was found to be larger (0.076 $m^3\ m^{-3}$) mainly due to the presence of a denser vegetation cover.

A significant result is related to the relatively low bias observed between SMOS L3SM product and ground-based soil moisture measurements. The calculated bias between ground-based soil moisture and SMOS product reveals a slight underestimation in the Mali and Niger sites (-0.003 and -0.010 $m^3\ m^{-3}$) and an overestimation of the SMOS product in the Benin site ($+0.039$ $m^3\ m^{-3}$). Previous studies (Al Bitar et al., 2012; Collow et al., 2012; dall'Amico et al., 2012) indicated that the SMOS soil moisture retrievals had a dry bias when compared to ground-based measurements; this does not seem to be the case in West Africa. It is worth noting that the slight overestimation of the SMOS soil moisture product in the Benin site is principally due to the uncertainty of the SMOS retrievals during the dry season (from December to April). During the rainy season, we can observe that the SMOS soil moisture product correctly reproduces the drying out periods observed between successive rainy events.

Another comment deals with the higher variability of the SMOS product compared to ground measurements. This behavior is mainly due to two effects. The first one is related to the soil depth sensitivity of the radiometric measurement which is known to be sensitive to the skin surface (basically 0–3 cm, but it can be 0–1 cm during a strong rainfall event) whereas soil moisture probes located at 5 cm depth are sensitive to the 2–8 cm soil layer. As shown in Fig. 3, soil moisture probe values hardly reach 0.3 $m^3\ m^{-3}$ whereas SMOS measurements exhibit higher values (up to 0.4 $m^3\ m^{-3}$ in Mali and Niger) and even higher in the Benin site (up to 0.73 $m^3\ m^{-3}$, not shown). This behavior also explains lower SMOS soil moisture values after a rain event which can be clearly observed on the three sites in Fig. 3. The second reason might be related to the uncertainty associated with the SMOS retrievals. The CATDS product provides the retrieved soil moisture value, and its associated data quality index (Dqx), not shown in Fig. 3 for readability reason. The mean Dqx value (2010–2012) is equal to 0.0052 $m^3\ m^{-3}$, 0.0037 $m^3\ m^{-3}$ and 0.0185 $m^3\ m^{-3}$ in Mali, Niger and Benin sites respectively. It is well known that the presence of vegetation at a given location increases the uncertainty of radiometric inversions (Pellarin et al., 2013) as shown by the mean Dqx value in the Benin site.

3.3. SMOS L3SM versus other satellite soil moisture products

Three other existing satellite-based soil moisture products were also considered to compare with SMOS L3SM product. Two products are based on the passive microwave AMSR-E instrument on-board of the AQUA platform: AMSR-E NSIDC (Njoku et al., 2003) and AMSR-E VUA (Owe et al., 2008). The AMSR-E NSIDC soil moisture product is based on the 10.7 and 18.7 GHz dual polarized frequencies whereas the AMSR-E VUA used in this study is obtained by applying the three parameter Land Parameter Retrieval Model to the dual polarized 6.9 GHz frequency. In order to ensure a good accuracy of the two products, only data of descending orbits, for which temperature gradient in the emitting layer are low, are used in this study (Gruhier et al., 2010). The third product (MetOp ASCAT, Bartalis et al., 2007) is derived from backscatter measurements acquired with the active ASCAT sensor onboard the three MetOp (Meteorological Operational) satellites. As this product provides soil moisture values scaled between 0 and 1 (representing zero soil moisture and saturation respectively), a rescaled procedure was used to obtain volumetric soil moisture content based on global soil texture maps. Thus, the ASCAT index (0–1) was simply multiplied by the saturated soil moisture value (θ_{sat}) derived from sand fraction over the three sites. The relationship between the saturated soil moisture value and the sand fraction is derived from the parameterization of the ISBA land surface model (Noilhan & Planton, 1989) and is given in Eq. (3) of the present paper (see Section 4.1). Statistical scores are presented in Table 2 and soil moisture time-series are presented in Fig. 4.

At the Mali site, the AMSR-E VUA and MetOp ASCAT soil moisture products obtain the best coefficient of correlation ($R = 0.82$) close to the SMOS product ($R = 0.74$). The AMSR-E NSIDC soil moisture products exhibit lower correlation coefficients ($R = 0.40$). Regarding the RMSE and bias scores, the SMOS product is in best agreement with ground measurements with lowest RMSE (0.033 $m^3\ m^{-3}$) and bias (-0.003 $m^3\ m^{-3}$) compared to AMSR-E products and MetOp ASCAT which obtain RMSE and bias scores higher that 0.04 $m^3\ m^{-3}$. Scores obtained at the Mali site are similar to those obtained in Gruhier et al. (2010). At the Niger site, the SMOS soil moisture product shows the best performances in terms of R, RMSE and bias. The AMSR-E VUA obtains a coefficient of correlation ($R = 0.69$) close to the SMOS product ($R = 0.70$) but lower scores in terms of RMSE and bias. MetOp ASCAT and AMSR-E NSIDC products obtain similar coefficients of correlation (0.52 and 0.58 respectively) and similar RMSE and bias scores. At the Benin site, the best coefficient of correlation ($R = 0.90$) is obtained by the MetOp ASCAT soil moisture product followed by the SMOS product ($R = 0.77$). The best RMSE and bias scores are obtained by the AMSR-E NSIDC product. In average over the three sites, the MetOp ASCAT product provides the best coefficient of correlation ($R = 0.746$) followed by the SMOS L3SM ($R = 0.736$), the AMSR-E VUA product ($R = 0.703$), and AMSR-E NSIDC product ($R = 0.523$). In terms of RMSE, the best agreement is obtained by the SMOS L3SM product (RMSE = 0.047 $m^3\ m^{-3}$), followed by the AMSR-E NSIDC product (RMSE = 0.063 $m^3\ m^{-3}$), the AMSR-E VUA product (RMSE = 0.088 $m^3\ m^{-3}$) and the MetOp ASCAT product (RMSE = 0.096 $m^3\ m^{-3}$).

Fig. 4 shows that the AMSR-E NSIDC, AMSR-E VUA and MetOp ASCAT satellite soil moisture products tend to overestimate soil moisture during dry seasons at the Mali and Niger sites whereas the SMOS product is able to correctly reproduce the low soil moisture values close to 0.01 $m^3\ m^{-3}$ (see Fig. 3). At the Benin site, SMOS also tends to overestimate soil moisture during dry seasons. Also shown in Fig. 4 is the timing delay of the MetOp ASCAT soil moisture product at the end of the rainy season when soil moisture measurements indicate a dry soil. This behavior is particularly evident at the Niger site and may

Table 2
Statistical results obtained between ground soil moisture measurements and four satellite products in Mali, Niger and Benin sites. *N* indicates the number of data (smaller for the Mali site (only 2010 year) and for the two AMSR-E products which stop in October 2011).

	Mali				Niger				Benin			
	N	*R*	RMSE	Bias	*N*	*R*	RMSE	Bias	*N*	*R*	RMSE	Bias
SMOS	289	0.74	0.033	−0.003	867	0.70	0.032	−0.010	870	0.77	0.076	0.039
AMSR-E NSIDC-asc	226	0.40	0.048	0.040	398	0.58	0.069	0.065	397	0.59	0.071	0.031
AMSR-E VUA-asc	87	0.82	0.056	0.043	143	0.69	0.044	0.021	353	0.60	0.166	0.120
ASCAT normalized	259	0.82	0.069	0.050	952	0.52	0.088	0.062	970	0.90	0.131	0.105

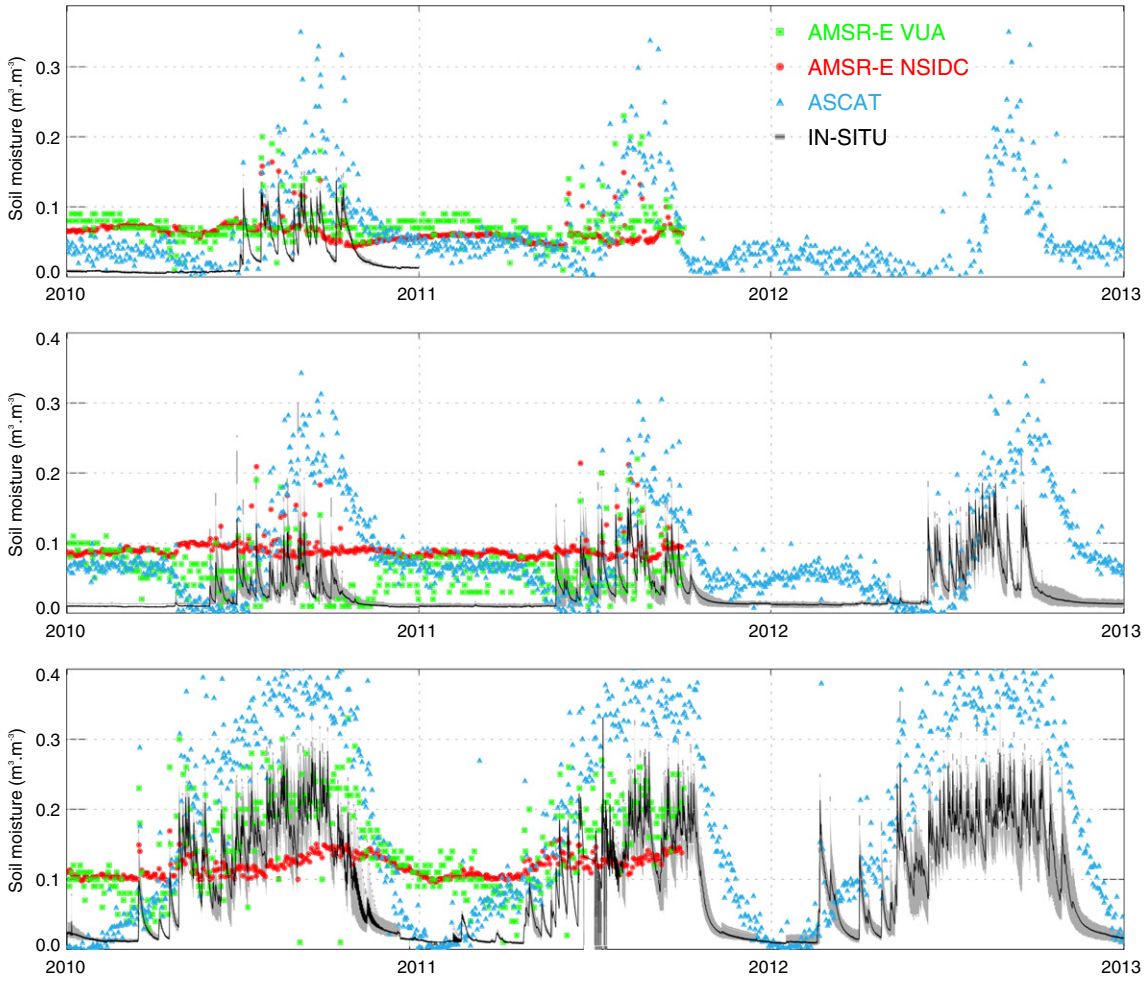

Fig. 4. Observed in-situ surface soil moisture (black curve) versus AMSR-E NSIDC (red circles), AMSR-E VUA (green square) and MetOp ASCAT (blue triangles) at the Mali (top), Niger (middle) and Benin (bottom) sites.

be due to the vegetation cover influence on the backscattering coefficient at C-band. The vegetation cover should also act on the backscattered signal over the Benin site.

4. Providing 3-hours soil moisture mapping in West Africa using SMOS

The SMOS mission was designed to provide a full global coverage of the earth every 3 days considering that, on most areas, surface soil moisture dynamic can be suitably captured at this temporal resolution. However, in arid and semi-arid regions, the dynamic of surface soil moisture can be very fast due to high evaporative rates. A consequence of the rapid drying-out of soils, the SMOS temporal resolution can be insufficient to catch each rainfall event. To solve this problem, the chosen solution consists on assimilating SMOS L3SM into a soil moisture model operating at a smaller temporal resolution.

Recently, Pellarin et al. (2013) developed a simple methodology aiming at retrieving soil moisture estimates between successive satellite soil moisture measurements in order to increase the temporal resolution. The methodology was initially developed for AMSR-E passive microwave measurements to correct satellite-based precipitation estimates (Pellarin, Laurent, et al., 2009a). In this section, we propose to apply the methodology to the SMOS soil moisture measurements.

4.1. API-mod semi-empirical model

The API-mod semi-empirical model (Pellarin et al., 2013) is based on the API (antecedent precipitation index) approach which was initially designed to provide a proxy of the surface soil moisture with a single precipitation observation. The API model can be expressed as:

$$\mathrm{API}(t) = \mathrm{API}(t_{-1}).e^{-\frac{\Delta t}{\tau}} + P(t) \quad (1)$$

where $P(t)$ is the rainfall accumulation (in mm) over a $\boldsymbol{\Delta t}$ period (in hour), and τ is a parameter which describes the soil drying-out velocity (in hour). The obtained API time-series is expressed in millimeter. To match the API with surface soil moisture measurements (expressed in $m^3\ m^{-3}$), a new semi-empirical relationship (API-mod) was developed and can be expressed as:

$$\mathrm{SSM}(t) = \mathrm{SSM}(t_{-1}) \cdot e^{-\frac{\Delta t}{\tau}} + [\theta_{\mathrm{sat}} - \mathrm{SSM}(t_{-1})] \cdot \left[1 - e^{-\frac{P(t)}{dsoil}}\right] + \theta_{\mathrm{res}} \quad (2)$$

where θ_{sat} ($m^3\ m^{-3}$) is the saturated soil moisture value, *dsoil* is the soil depth (in mm) and θ_{res} ($m^3\ m^{-3}$) is the "residual" surface soil moisture. When there is no rain, the second term of Eq. (2) is equal to zero and $\mathrm{SSM}(t)$ decreases exponentially with time to θ_{res} value. When there is a rain event, SSM increases proportionally to the rainrate $P(t)$, and the

model also depends on the previous soil storage capacity expressed as $[\theta_{sat} - SSM(t-1)]$. Furthermore, the SSM increase during a rain event depends upon the considered soil depth *dsoil* since the first top few centimeters of soil is expected to increase faster than deeper soil layers. *dsoil* was set to 100 mm (i.e. 0–10 cm soil layer) to compare with ground-based soil moisture, and set to 50 mm (i.e. 0–5 cm soil layer) to compare with satellite-based soil moisture product. θ_{sat} ($m^3\ m^{-3}$) is the saturated soil water content and was derived from the parameterization of the ISBA land surface model (Noilhan & Planton, 1989) as:

$$\theta_{sat} = 0.001 \times (-108 \times sand + 494.305) \quad (3)$$

with *sand* is the sand soil fraction between 0 and 1. The τ value describes the drying-out velocity and was found (in a first approximation) to be dependent on the clay fraction (Pellarin et al., 2013) as:

$$\tau_{(0-10\ cm)} = 32 \times \ln(clay) + 174 \quad (4)$$

In the present study, there is only one difference with the previous algorithm developed in Pellarin et al. (2013). Arbitrary fixed to 0.01 $m^3\ m^{-3}$ in the previous study, the θ_{res} parameter is now determined using the mean value of the 30 lowest SMOS soil moisture retrievals during the 2010–2012 period. This permits to get a spatial distribution of the θ_{res} parameter ranging from 0.001 $m^3\ m^{-3}$ in the Sahara region to 0.11 $m^3\ m^{-3}$ for instance in Guinea and Sierra Leone.

4.2. SMOS assimilation into the API-mod model

The API-mod model is able to provide soil moisture estimates in $m^3\ m^{-3}$. Thus it is possible to assimilate the SMOS L3SM product. The proposed approach described in Pellarin et al. (2013) is two-steps: (i) compute soil moisture time-series using the API-mod model and a satellite-based precipitation product (CMORPH, TRMM-3B42 or PERSIANN) and (ii) compare simulated soil moisture with observations (SMOS) in order to adjust the precipitation rate to reduce the differences between simulated and observed soil moisture. It can be seen as a simple assimilation scheme. One output of this algorithm is the best soil moisture time-series (called API-mod*). Previous results obtained at C-band with AMSR-E sensor show a systematic improvement of soil moisture time-series. However, it was found that the efficiency of the methodology was better in the Sahelian region (Mali and Niger) than in the Soudanian region (Benin). This was found to be due to the denser vegetation cover in Benin which strongly attenuates the soil emission at C-band.

The assimilation of the SMOS measurements into the API-mod model is simpler than in Pellarin et al. (2013). In the last study, the soil moisture product used (NASA-AMSR-E product, Njoku et al., 2003) was found to be biased compared to ground-based soil moisture measurements. To solve this, we had to consider raw brightness temperatures instead of soil moisture product which involving computing TB with a microwave radiative model. As the SMOS L3SM was found to be reasonably unbiased (Section 3.2 of the present study), it was possible to directly use the SMOS soil moisture retrievals in our methodology.

The basic operation of the methodology can be illustrated in Fig. 5. Based on a precipitation time-series (for instance a satellite-based precipitation product), it is possible to derive a soil moisture time-series using a simple semi-empirical model (API-mod, Eq. 2). At this stage, the accuracy of the obtained soil moisture time-series is not essential. During a given time-period defined either by two successive rain events or by seven successive days (September 22nd to 29th in the example presented in Fig. 5), there are few SMOS soil moisture retrievals (five in this example). The method consists on computing different soil moisture time-series using Eq. (2) associated with different rain rates (based on various multiplicative factors applied to satellite-based precipitation rate). The best solution is given by the soil moisture simulation which

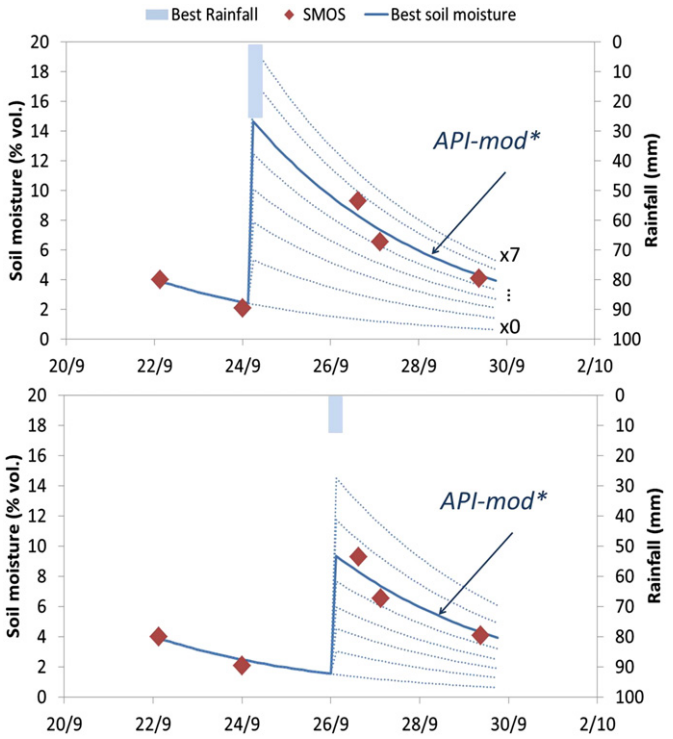

Fig. 5. Illustration of the methodology developed to retrieve surface soil moisture estimates between successive satellite measurements. The knowledge of the rainfall date permits to reproduce the real soil moisture temporal evolution.

minimizes the RMSE between simulated soil moisture and SMOS product (the best soil moisture time-series is called API-mod*). This methodology can be seen as a simple assimilation scheme. The knowledge of the rainfall date is crucial to ensure accurate retrieval of soil moisture dynamics. If not, given the five SMOS soil moisture estimates illustrated in Fig. 5, it is not possible to choose between either a strong rain event (associated with a significant evolution of the soil moisture, top graph) or a weak rain event (associated with a small evolution of the soil moisture, bottom graph). Thus, the methodology exploits the rainfall date provided by a satellite-based precipitation product rather than its quantitative estimate. Prior tests show that precipitation products provide generally good skills to state when it is raining in West Africa since most of rainfall events are of convective type and, consequently, easy to detect with satellite algorithms.

To resume, on a given $25 \times 25\ km^2$ pixel, the algorithm is applied to each period (either defined by two successive rainfall events or a fixed period of 7 days), and to repeat this over all pixels in West Africa. Concretely, the methodology consists on performing eight soil moisture simulations using multiplicative factors ($\times 0$, $\times 0.25$, $\times 0.5$, $\times 1$, $\times 2$, $\times 3$, $\times 5$, $\times 7$) applied on the original precipitation estimates. The best solution is the multiplicative factor that provides the best fit between simulated and SMOS L3SM soil moisture estimates (in terms of RMSE).

The assimilation of SMOS L3SM product into the API-mod model was done over the whole West Africa region and evaluated over the three sites located in Mali, Niger and Benin. A sensitivity analysis was conducted to assess the influence of the satellite-based precipitation products used in this study (CMORPH, TRMM-3B42 and PERSIANN). Results obtained in Mali, Niger and Benin are shown in Fig. 6. In this example, the PERSIANN precipitation product is used together with SMOS assimilation. Corresponding statistical scores are shown in Fig. 6 and reported in Table 3. Other satellite precipitation products (CMORPH and TRMM-3B42) were used and corresponding statistical scores related to API-mod performance with SMOS assimilation are given in Table 3.

Globally, the SMOS L3SM assimilation into the API-mod model provides accurate soil moisture estimates with RMSE scores better that the

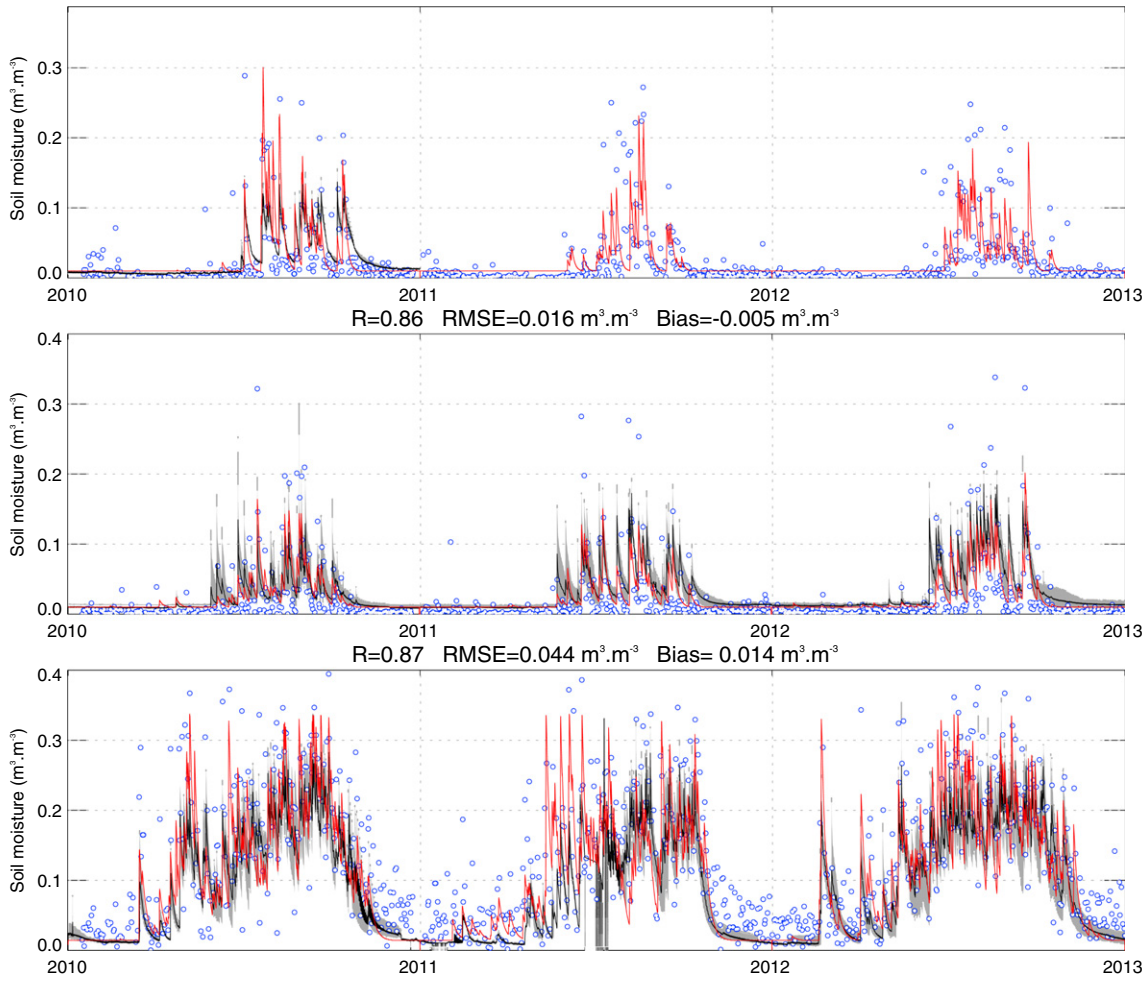

Fig. 6. Observed surface soil moisture (black curve) versus estimated surface soil moisture (API-mod* using PERSIANN, red curve) at the Mali (top), Niger (middle) and Benin (bottom) sites. Open blue circles are SMOS L3SM soil moisture estimates. Scores on top graphs are related to ground-based measurements versus API-mod* surface soil moisture estimates.

0.04 $m^3\ m^{-3}$ target accuracy of SMOS except for the Benin site using the PERSIANN product (0.044 $m^3\ m^{-3}$). Correlation coefficient scores over the three sites always exceed 0.8 and are generally close to 0.9. The bias is also reduced mainly in the Benin site due to the correction of the overestimation during the dry season observed with SMOS L3SM (Fig. 6). Compared to SMOS L3SM, the methodology improves all scores by about 10–15%. An important result concerns the convergence of all API-mod* time-series whatever the satellite precipitation product used as input of the methodology. This result indicates that we can use indifferently one of the three precipitation products without changing so much the accuracy of the retrieved 3-hourly soil moisture product.

Table 3 also presents statistical scores obtained by the API-mod model without SMOS soil moisture assimilation. Depending on the precipitation product used, it can be observed that the API-mod soil moisture scores can be either better or worse than the SMOS L3SM product. In addition, based on Table 3, it is not possible to designate which is the best precipitation product. For instance, the correlation coefficient obtained with PERSIANN product in Mali is 0.82 but only 0.63 in Benin. On the contrary, the correlation coefficient obtained with TRMM-3B42 in Benin is 0.84 but only 0.76 in the Mali site. This large dispersion of the scores, related to the choice of the precipitation product, is not observed when SMOS L3SM estimates are assimilated into the API-mod model as shown in Table 3.

Table 3
Statistical scores between ground-based soil moisture measurements and SMOS L3SM (first line) and API-mod* soil moisture estimates with and without SMOS assimilation. The influence of various precipitation products (PERSIANN, CMORPH and TRMM-3B42) on the API-mod is presented.

	2010–2012	Mali (only 2010)			Niger			Benin		
		R	RMSE	Bias	*R*	RMSE	Bias	*R*	RMSE	Bias
	SMOS	0.74	0.033	−0.003	0.70	0.032	−0.010	0.77	0.076	0.039
API-mod* without SMOS	PERSIANN	0.82	0.034	0.009	0.79	0.054	0.025	0.63	0.063	0.002
	CMORPH	0.84	0.023	−0.013	0.78	0.016	−0.004	0.75	0.067	−0.041
	TRMM3B42	0.76	0.021	−0.008	0.80	0.021	0.000	0.84	0.046	−0.021
API-mod* with SMOS	PERSIANN	0.82	0.025	0.000	0.86	0.016	−0.005	0.87	0.044	0.014
	CMORPH	0.82	0.029	0.001	0.85	0.015	−0.002	0.89	0.036	0.008
	TRMM3B42	0.85	0.026	0.001	0.83	0.018	−0.004	0.89	0.038	0.010

Another interesting result can be observed at the regional scale. Fig. 7 shows three soil moisture maps obtained at the same date (September 13th 2011, 0600 LST). The first one is obtained using Eq. (2) with PERSIANN product but without SMOS L3SM assimilation. The second graph shows the SMOS retrieved L3SM for ascending pass at 0600 LST. The third graph is obtained using Eq. (2) with PERSIANN product and SMOS L3SM assimilation (API-mod*). The first comment deals with the overall smoother variability of the first graph versus second and third graphs. The smoother soil moisture variability is directly related to the rainfall spatial variability signature. As satellite-based precipitation products are mainly based on the detection of cloud temperatures (using thermal infrared measurements), it is quite difficult to distinguish where rain occurs under a large cloudy system. On the contrary, passive microwave of SMOS (middle graph in Fig. 7) is not sensitive to cloud properties but only to the soil emission (mainly driven by the surface soil moisture and the vegetation water content), i.e. where the rainfall reached the soil. During and immediately after a rain event, the spatial variability of SMOS L3SM product is expected to better capture the spatial variability of the precipitation.

The bottom graph of Fig. 7 (API-mod*) displays improved soil moisture estimates in areas outside the swath. This is due to the assimilation scheme which uses various SMOS measurements over periods of few days in order to adjust soil moisture estimates. Last graph of Fig. 7 shows that the soil moisture spatial variability is quite similar to that of the SMOS L3SM product. The advantage of the proposed methodology is to obtain regional soil moisture maps every 3 hours which respect the spatial variability of SMOS measurements. This product can be downloaded on the website: http://bd.amma-catch.org/amma-catch2/main.jsf.

The last example is shown in Fig. 8 to illustrate typical differences in terms of spatial variability of surface soil moisture estimates. July 5th 2011, 1800 LST, a large convective system reached the South-Western of Niger. Fig. 8 (left) presents the soil moisture patch obtained using Eq. (2) with PERSIANN precipitation product without SMOS L3SM assimilation. It indicates that the rainfall event affects the main part of South-Western Niger. On the other hand, the middle and right graphs (SMOS L3SM, and Eq. (2) with PERSIANN and SMOS L3SM assimilation respectively) define a smaller soil moisture patch which seems to

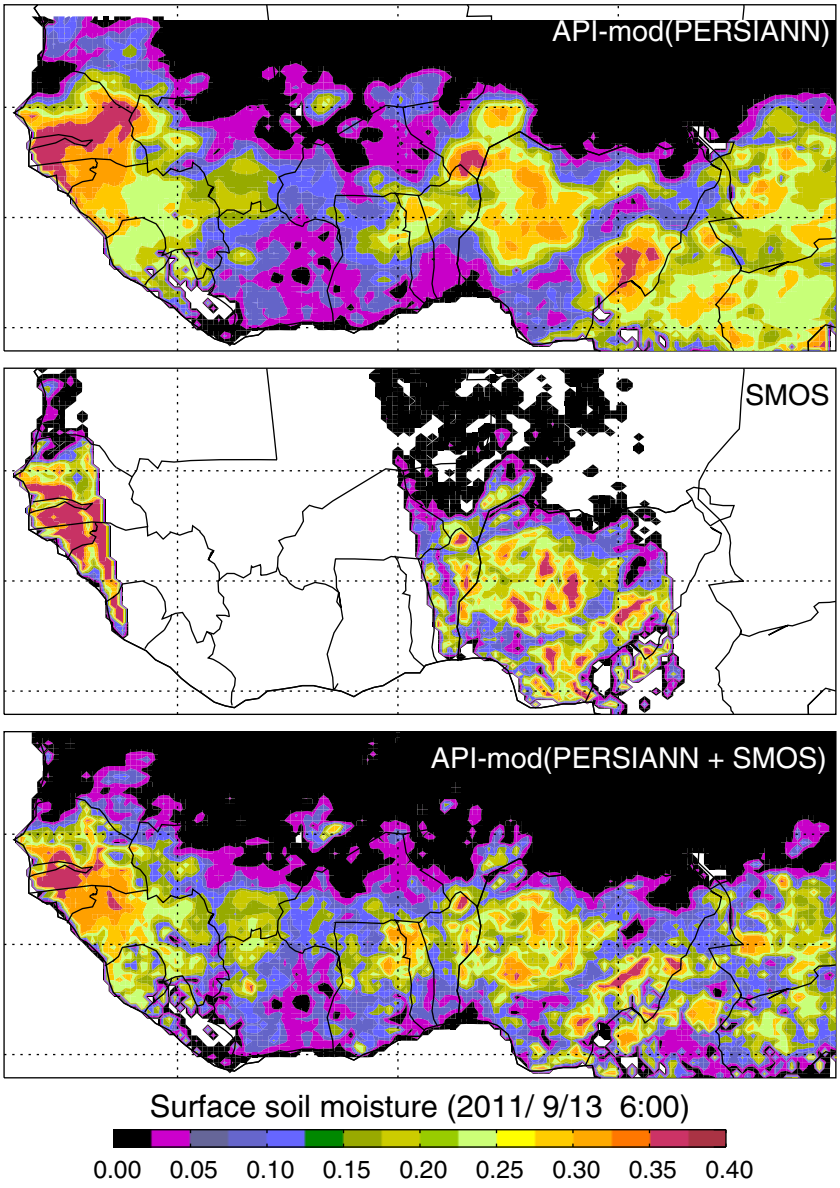

Fig. 7. Surface soil moisture mapping (September, 13th, 2011) using API-mod model without SMOS measurements (top graph), SMOS L3SM product (middle graph) and API-mod model with SMOS measurements (bottom graph).

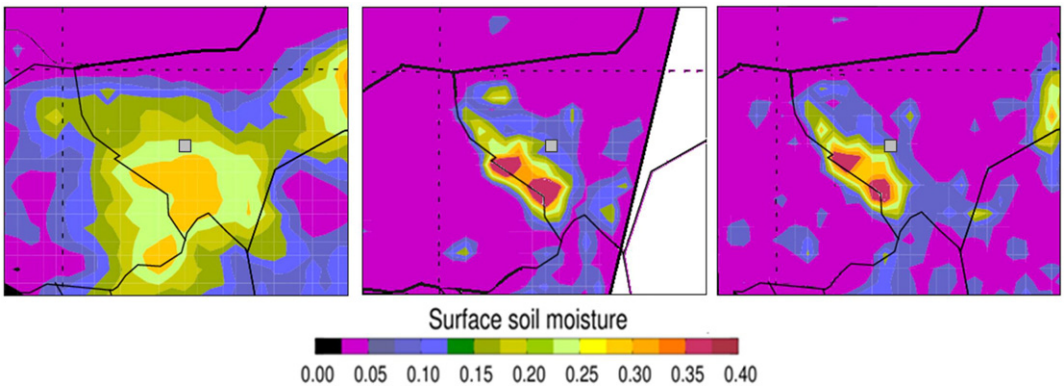

Fig. 8. Typical example of soil moisture patches provided by the API-mod model without SMOS assimilation (left graph), SMOS L3SM soil moisture retrievals (middle graph) and API-mod model with SMOS assimilation (right graph). This was obtained for July, 5th 2011, 1800 LST, South-West Niger area.

indicate that the convective system provides precipitation mainly at the border between Burkina Faso and Niger. Otherwise, the shape of soil moisture patch is consistent with typical squall lines observed in West Africa.

For this particular precipitation event, we compared ground observations with satellite estimates of soil moisture and precipitation over the 0.25° pixel in the Niger site (square symbol in Fig. 8). The PERSIANN satellite precipitation products indicated 41 mm whereas the rainfall amount measured at the ground station was 17 mm. Regarding soil moisture, ground soil moisture measurements were maximum at 1800 LST and equal to 0.113 $m^3\ m^{-3}$ whereas the API-mod model without SMOS assimilation indicated 0.247 $m^3\ m^{-3}$. The SMOS L3SM product indicated 0.082 $m^3\ m^{-3}$. Finally, the API-mod model with SMOS assimilation indicated 0.082 $m^3\ m^{-3}$ (with PERSIANN product, right graph Fig. 8), 0.129 $m^3\ m^{-3}$ (with CMORPH product) and 0.133 $m^3\ m^{-3}$ (with TRMM-3B42 product).

5. Conclusion

This paper assessed the SMOS soil moisture values from Level 3 product provided by the CATDS (version 2.4 and 2.5) and available on the website http://www.catds.fr/. The evaluation was conducted at the local scale through comparison with ground-based soil moisture measurements acquired in Mali, Niger and Benin from 2010 to 2012. Computed correlation coefficients (R) were found to be equal to 0.74, 0.70 and 0.77 respectively for the Mali, Niger and Benin sites. RMSE scores were found to be better than the SMOS expected soil moisture retrieval accuracy (fixed to 0.04 $m^3\ m^{-3}$) in the Niger and Mali sites (0.032 $m^3\ m^{-3}$ and 0.033 $m^3\ m^{-3}$ respectively). On the other hand, the RMSE score in the Benin site was found to be larger (0.076 $m^3\ m^{-3}$) mainly due to the presence of a denser vegetation cover. An important result is related to the low dry bias between ground-based and SMOS L3SM soil moisture in low vegetated areas (Mali and Niger site) and a weak wet-bias was found in the Benin site (0.039 $m^3\ m^{-3}$) but is mainly due to overestimation of the L3SM product during the dry season.

A comparison with other satellite-based soil moisture products was done in Mali, Niger and Benin. In average over the three sites, the SMOS L3SM product provided the best agreement in terms of RMSE (RMSE = 0.047 $m^3\ m^{-3}$), followed by the AMSR-E NSIDC product (RMSE = 0.063 $m^3\ m^{-3}$), the AMSR-E VUA product (RMSE = 0.088 $m^3\ m^{-3}$) and the MetOp ASCAT product (RMSE = 0.096 $m^3\ m^{-3}$). However, the MetOp ASCAT product was found to have the best correlation coefficient in average over the three sites.

A simple assimilation scheme was proposed in order to compute regional scale 3-hour soil moisture maps over the whole West Africa region. Based on a simple semi-empirical relationship (API-mod) and a satellite-based precipitation product, SMOS L3SM product was used to obtain 3-hour regional soil moisture mapping. The proposed methodology led to improve the SMOS L3SM product over the three local sites. Improvement, in terms of RMSE scores, was found to be equal to 24% in Mali, 50% in Niger and 42% in Benin (using PERSIANN product). In terms of coefficient of correlation, the improvement was 10%, 19% and 11% in Mali, Niger and Benin respectively. In addition, one particular interest of the proposed methodology was to provide 3-hour regional soil moisture mapping over West Africa which can be useful for agricultural applications, drought detection or flood warning. As the methodology requires only SMOS L3SM and a satellite precipitation product, a near-real time 3-hour soil moisture product can be envisaged. Currently, the 3-hour soil moisture mapping is used as a new constrain for interpolating local precipitation measurements in order to provide more realistic spatial krigged precipitation mapping in West Africa.

Acknowledgment

The ground validation data set was obtained in the framework of the AMMA (African Monsoon Multidisciplinary Analysis) Program and the AMMA-CATCH observatory (www.amma-catch.org). Based on a French initiative, AMMA was built by an international scientific group and is currently funded by a large number of agencies, especially from France, UK, US and Africa. It has been the beneficiary of a major financial contribution from the European Community Sixth Framework Research Program. Detailed information on scientific coordination and funding is available on the AMMA International web site http://www.amma-international.org. This study received financial support by TOSCA (CNES, Centre National d'Etudes Spatiales, France) and ESA (European Space Agency) in the framework of the cal/val activities of the SMOS mission. A particular thanks to Monique Oï, Ibrahim Mainassara, Abdoulaye Kone, Aliko Maman, Hamissou Alassane, Vanessa Bentahar, Sarah Soubeyran, Stephane Boubkraoui and Max Wubda for having provided us with ground measurements in instable security context. Acknowledgments also to the Land Surface Analysis Satellite Applications Facility (LSA SAF) for providing us with the MSG-SEVIRI LAI product.

References

Adler, B., Kalthoff, N., & Gantner, L. (2011). The impact of soil moisture inhomogeneities on the modification of a mesoscale convective system: An idealised model study. *Atmospheric Research*, *101*, 354–372.

Al Bitar, A., Leroux, D., Kerr, Y.H., Merlin, O., Richaume, P., Sahoo, A., et al. (2012). Evaluation of SMOS soil moisture products over continental US using the SCAN/SNOTEL Network. *IEEE Transactions on Geoscience and Remote Sensing*, *50*, 1572–1586.

Albergel, C., de Rosnay, P., Gruhier, C., Munoz-Sabater, J., Hasenauer, S., Isaksen, L., et al. (2012). Evaluation of remotely sensed and modelled soil moisture products using

global ground-based in situ observations. *Remote Sensing of Environment*, *118*, 215–226.
Al-Yaari, A., Wigneron, J. -P., Ducharne, A., Kerr, Y.H., de Rosnay, P., de Jeu, R., et al. (2014). Global-scale evaluation of two satellite-based passive microwave soil moisture datasets (SMOS and AMSR-E) with respect to Land Data Assimilation System estimates. *Remote Sensing of Environment*, *149*, 181–195.
Bartalis, Z., Wagner, W., Naeimi, V., Hasenauer, S., Scipal, K., Bonekamp, H., et al. (2007). Initial soil moisture retrievals from the METOP-A Advanced Scatterometer (ASCAT). *Geophysical Research Letters*, *34*.
Baup, F., Mougin, E., de Rosnay, P., Hiernaux, P., Frappart, F., Frison, P.L., et al. (2011). Mapping surface soil moisture over the Gourma mesoscale site (Mali) by using ENVISAT ASAR data. *Hydrology and Earth System Sciences*, *15*, 603–616.
Baup, F., Mougin, E., de Rosnay, P., Timouk, F., & Chenerie, I. (2007). Surface soil moisture estimation over the AMMA Sahelian site in Mali using ENVISAT/ASAR data. *Remote Sensing of Environment*, *109*, 473–481.
Bircher, S., Skou, N., Jensen, K.H., Walker, J.P., & Rasmussen, L. (2012). A soil moisture and temperature network for SMOS validation in Western Denmark. *Hydrology and Earth System Sciences*, *16*, 1445–1463.
Brocca, L., Tullo, T., Melone, F., Moramarco, T., & Morbidelli, R. (2012). Catchment scale soil moisture spatial-temporal variability. *Journal of Hydrology*, *422*, 63–75.
Cappelaere, B., Descroix, L., Lebel, T., Boulain, N., Ramier, D., Laurent, J.P., et al. (2009). The AMMA-CATCH experiment in the cultivated Sahelian area of south-west Niger — investigating water cycle response to a fluctuating climate and changing environment. *Journal of Hydrology*, *375*, 34–51.
Collow, T.W., Robock, A., Basara, J.B., & Illston, B.G. (2012). Evaluation of SMOS retrievals of soil moisture over the central United States with currently available in situ observations. *Journal of Geophysical Research-Atmospheres*, *117*.
Cosh, M.H., Jackson, T.J., Bindlish, R., & Prueger, J.H. (2004). Watershed scale temporal and spatial stability of soil moisture and its role in validating satellite estimates. *Remote Sensing of Environment*, *92*, 427–435.
dall'Amico, J.T., Schlenz, F., Loew, A., & Mauser, W. (2012). First results of SMOS soil moisture validation in the Upper Danube catchment. *IEEE Transactions on Geoscience and Remote Sensing*, *50*, 1507–1516.
de Rosnay, P., Gruhier, C., Timouk, F., Baup, F., Mougin, E., Hiernaux, P., et al. (2009). Multi-scale soil moisture measurements at the Gourma meso-scale site in Mali. *Journal of Hydrology*, *375*, 241–252.
Dobson, M.C., Ulaby, F.T., Hallikainen, M.T., & El-Rayes, M.A. (1985). Microwave dielectric behavior of wet soil—part II. *Dielectric Mixing Models*, *GE-23*, 35–46.
Eltahir, E.A.B. (1998). A soil moisture rainfall feedback mechanism 1. Theory and observations. *Water Resources Research*, *34*, 765–776.
Escorihuela, M.J., Chanzy, A., Wigneron, J.P., & Kerr, Y.H. (2010). Effective soil moisture sampling depth of L-band radiometry: A case study. *Remote Sensing of Environment*, *114*, 995–1001.
Fatras, C., Frappart, F., Mougin, E., Grippa, M., & Hiernaux, P. (2012). Estimating surface soil moisture over Sahel using ENVISAT radar altimetry. *Remote Sensing of Environment*, *123*, 496–507.
Fischer, E.M., Seneviratne, S.I., Vidale, P.L., Luthi, D., & Schar, C. (2007). Soil moisture — atmosphere interactions during the 2003 European summer heat wave. *Journal of Climate*, *20*, 5081–5099.
Gosset, M., Viarre, J., Quantin, G., & Alcoba, M. (2013). Evaluation of several rainfall products used for hydrological applications over West Africa using two high-resolution gauge networks. *Quarterly Journal of the Royal Meteorological Society*, *139*, 923–940.
Gruhier, C., de Rosnay, P., Hasenauer, S., Holmes, T., de Jeu, R., Kerr, Y., et al. (2010). Soil moisture active and passive microwave products: Intercomparison and evaluation over a Sahelian site. *Hydrology and Earth System Sciences*, *14*, 141–156.
Gruhier, C., de Rosnay, P., Kerr, Y., Mougin, E., Ceschia, E., Calvet, J.C., et al. (2008). Evaluation of AMSR-E soil moisture product based on ground measurements over temperate and semi-arid regions. *Geophysical Research Letters*, *35*.
Jackson, T.J., Bindlish, R., Cosh, M.H., Zhao, T.J., Starks, P.J., Bosch, D.D., et al. (2012). Validation of Soil Moisture and Ocean Salinity (SMOS) soil moisture over watershed networks in the U.S. *IEEE Transactions on Geoscience and Remote Sensing*, *50*, 1530–1543.
Joyce, R.J., Janowiak, J.E., Arkin, P.A., & Xie, P.P. (2004). CMORPH: A method that produces global precipitation estimates from passive microwave and infrared data at high spatial and temporal resolution. *Journal of Hydrometeorology*, *5*, 487–503.
Kerr, Y.H. (2007). Soil moisture from space: Where are we? *Hydrogeology Journal*, *15*, 117–120.
Kerr, Y.H., Waldteufel, P., Richaume, P., Wigneron, J.P., Ferrazzoli, P., Mahmoodi, A., et al. (2012). The SMOS soil moisture retrieval algorithm. *IEEE Transactions on Geoscience and Remote Sensing*, *50*, 1384–1403.
Kerr, Y.H., Waldteufel, P., Wigneron, J.P., Martinuzzi, J.M., Font, J., & Berger, M. (2001). Soil moisture retrieval from space: The Soil Moisture and Ocean Salinity (SMOS) mission. *IEEE Transactions on Geoscience and Remote Sensing*, *39*, 1729–1735.
Klupfel, V., Kalthoff, N., Gantner, L., & Kottmeier, C. (2011). Evaluation of soil moisture ensemble runs to estimate precipitation variability in convection-permitting model simulations for West Africa. *Atmospheric Research*, *101*, 178–193.
Koster, R.D., Dirmeyer, P.A., Guo, Z.C., Bonan, G., Chan, E., Cox, P., et al. (2004). Regions of strong coupling between soil moisture and precipitation. *Science*, *305*, 1138–1140.
Kummerow, C., Hong, Y., Olson, W.S., Yang, S., Adler, R.F., McCollum, J., et al. (2001). The evolution of the Goddard profiling algorithm (GPROF) for rainfall estimation from passive microwave sensors. *Journal of Applied Meteorology*, *40*, 1801–1820.
Lacava, T., Matgen, P., Brocca, L., Bittelli, M., Pergola, N., Moramarco, T., et al. (2012). A first assessment of the SMOS soil moisture product with in situ and modeled data in Italy and Luxembourg. *IEEE Transactions on Geoscience and Remote Sensing*, *50*, 1612–1622.
Lebel, T., Cappelaere, B., Galle, S., Hanan, N., Kergoat, L., Levis, S., et al. (2009). AMMA-CATCH studies in the Sahelian region of West-Africa: An overview. *Journal of Hydrology*, *375*, 3–13.
Leroux, D.J., Kerr, Y.H., Al Bitar, A., Bindlish, R., Jackson, T.J., Berthelot, B., et al. (2014). Comparison between SMOS, VUA, ASCAT, and ecmwf soil moisture products over four watersheds in US. *IEEE Transactions on Geoscience and Remote Sensing*, *52*(3), 1562–1571.
Leroux, D.J., Kerr, Y.H., Richaume, P., & Fieuzal, R. (2013). Spatial distribution and possible sources of SMOS errors at the global scale. *Remote Sensing of Environment*, *133*, 240–250.
Loew, A., & Schlenz, F. (2011). A dynamic approach for evaluating coarse scale satellite soil moisture products. *Hydrology and Earth System Sciences*, *15*, 75–90.
Miralles, D.G., Crow, W.T., & Cosh, M.H. (2010). Estimating spatial sampling errors in coarse-scale soil moisture estimates derived from point-scale observations. *Journal of Hydrometeorology*, *11*, 1423–1429.
Montzka, C., Bogena, H.R., Weihermuller, L., Jonard, F., Bouzinac, C., Kainulainen, J., et al. (2013). Brightness temperature and soil moisture validation at different scales during the SMOS validation campaign in the Rur and Erft Catchments, Germany. *IEEE Transactions on Geoscience and Remote Sensing*, *51*, 1728–1743.
Mougin, E., Hiernaux, P., Kergoat, L., Grippa, M., de Rosnay, P., Timouk, F., et al. (2009). The AMMA-CATCH Gourma observatory site in Mali: Relating climatic variations to changes in vegetation, surface hydrology, fluxes and natural resources. *Journal of Hydrology*, *375*, 14–33.
Njoku, E.G., Jackson, T.J., Lakshmi, V., Chan, T.K., & Nghiem, S.V. (2003). Soil moisture retrieval from AMSR-E. *IEEE Transactions on Geoscience and Remote Sensing*, *41*, 215–229.
Noilhan, J., & Planton, S. (1989). A simple parameterization of land surface processes for meteorological models. *Monthly Weather Review*, *117*, 536–549.
Owe, M., de Jeu, R., & Holmes, T. (2008). Multisensor historical climatology of satellite-derived global land surface moisture. *Journal of Geophysical Research-Earth Surface*, *113*.
Parrens, M., Zakharova, E., Lafont, S., Calvet, J.C., Kerr, Y., Wagner, W., et al. (2012). Comparing soil moisture retrievals from SMOS and ASCAT over France. *Hydrology and Earth System Sciences*, *16*, 423–440.
Peischl, S., Walker, J.P., Rudiger, C., Ye, N., Kerr, Y.H., Kim, E., et al. (2012). The AACES field experiments: SMOS calibration and validation across the Murrumbidgee River catchment. *Hydrology and Earth System Sciences*, *16*, 1697–1708.
Pellarin, T., Laurent, J.P., Cappelaere, B., Decharme, B., Descroix, L., & Ramier, D. (2009). Hydrological modelling and associated microwave emission of a semi-arid region in South-western Niger. *Journal of Hydrology*, *375*, 262–272.
Pellarin, T., Louvet, S., Gruhier, C., Quantin, G., & Legout, C. (2013). A simple and effective method for correcting soil moisture and precipitation estimates using AMSR-E measurements. *Remote Sensing of Environment*, *136*, 28–36.
Pellarin, T., Tran, T., Cohard, J.M., Galle, S., Laurent, J.P., de Rosnay, P., et al. (2009). Soil moisture mapping over West Africa with a 30-min temporal resolution using AMSR-E observations and a satellite-based rainfall product. *Hydrology and Earth System Sciences*, *13*, 1887–1896.
Pierdicca, N., Pulvirenti, L., Fascetti, F., Crapolicchio, R., & Talone, M. (2013). Analysis of two years of ASCAT- and SMOS-derived soil moisture estimates over Europe and North Africa. *European Journal of Remote Sensing*, *46*, 759–773.
Schlenz, F., dall'Amico, J.T., Mauser, W., & Loew, A. (2012). Analysis of SMOS brightness temperature and vegetation optical depth data with coupled land surface and radiative transfer models in Southern Germany. *Hydrology and Earth System Sciences*, *16*, 3517–3533.
Seguis, L., Kamagate, B., Favreau, G., Descloitres, M., Seidel, J.L., Galle, S., et al. (2011). Origins of streamflow in a crystalline basement catchment in a sub-humid Sudanian zone: The Donga basin (Benin, West Africa) Inter-annual variability of water budget. *Journal of Hydrology*, *402*, 1–13.
Sorooshian, S., Hsu, K.L., Gao, X., Gupta, H.V., Imam, B., & Braithwaite, D. (2000). Evaluation of PERSIANN system satellite-based estimates of tropical rainfall. *Bulletin of the American Meteorological Society*, *81*, 2035–2046.
Taylor, C.M., Gounou, A., Guichard, F., Harris, P.P., Ellis, R.J., Couvreux, F., et al. (2011). Frequency of Sahelian storm initiation enhanced over mesoscale soil-moisture patterns. *Nature Geoscience*, *4*, 430–433.
Vischel, T., Quantin, G., Lebel, T., Viarre, J., Gosset, M., Cazenave, F., et al. (2011). Generation of high-resolution rain fields in West Africa: Evaluation of dynamic interpolation methods. *Journal of Hydrometeorology*, *12*, 1465–1482.
Wigneron, J.P., Kerr, Y., Waldteufel, P., Saleh, K., Escorihuela, M.J., Richaume, P., et al. (2007). L-band Microwave Emission of the Biosphere (L-MEB) Model: Description and calibration against experimental data sets over crop fields. *Remote Sensing of Environment*, *107*, 639–655.
Wigneron, J. -P., Schwank, M., Lopez Baeza, E., Kerr, Y., Novello, N., Millan, C., et al. (2012). First evaluation of the simultaneous SMOS and ELBARA-II observations in the Mediterranean region. *Remote Sensing of Environment*, *124*, 26–37.
Zribi, M., Parde, M., De Rosnay, P., Baup, F., Boulain, N., Descroix, L., et al. (2009). ERS scatterometer surface soil moisture analysis of two sites in the south and north of the Sahel region of West Africa. *Journal of Hydrology*, *375*, 253–261.